

COMPOSITION AND SIZE-CONTROLLED SYNTHESIS OF Gd-DOPED MnZn FERRITE NANOCRYSTALS

O. Perales-Perez¹, E. Calderón-Ortiz², and S. Urcia-Romero³

¹Department of Engineering Science & Materials, University of Puerto Rico, Mayagüez, PR 00681-9044

²School of Science and Technology, Turabo University, Gurabo PR 00778-3030

³Department of Physics, University of Puerto Rico, Mayagüez, PR 00681-9044

E-mail: ojuan@uprm.edu. Phone (787)832-4040 x3071. Fax (787)265-3816

ABSTRACT

The use of ferromagnetic fluids for cooling applications represents an encouraging alternative to traditional methods; the fact that the fluid can be pumped with no moving mechanical parts, using the magnetocaloric effect, can be a great advantage for many applications where maintenance or power consumption are undesirable. A magnetic material suitable for this application has to fulfill certain requirements like tunable demagnetization temperature (T_c), high saturation magnetization (M_s) and high enough pyromagnetic coefficient ($\Delta M/\Delta T$). On this basis, the present work is focused on the synthesis of pure and Gd-doped $Mn_xZn_{1-x}Fe_2O_4$ nanoparticles as candidate materials for magnetocaloric pumping applications. The synthesis of the ferrite nanoparticles was carried out by a modified coprecipitation approach where the oversaturation in the reacting solution was controlled by the addition of reactants at specific flow-rates.

Keywords: Gd-doped MnZn ferrite, nanocrystals, size-controlled synthesis, demagnetization temperature, pyromagnetic coefficient.

INTRODUCTION

The fundamentals of magnetocaloric pumping can be traced back to the early work of Rosensweig [1], whose calculations suggested the possibility of pumping a magnetic fluid using only its thermal and magnetic properties. Magnetic materials tend to lose their magnetization as their temperature approximates their specific demagnetization point (T_c). Then, by exposing fluid hosting magnetic nanoparticles to a uniform and constant magnetic field, coincident with a changing temperature, a pressure gradient will be induced. As this magnetic fluid heats up, it loses its attraction to the magnetic field and gets displaced by the cooler volume fraction [2]. The impact of such a phenomenon is obvious: fluid propulsion with nonmoving mechanical parts [1-4]. A magnetic material suitable for this application should exhibit tunable demagnetization temperature (T_c) coupled with a high saturation magnetization (M_s) and pyromagnetic coefficient ($\Delta M/\Delta T$). Mn-Zn ferrite is considered a material that fulfills most of the previously mentioned requirements [5]. The replacement of Mn ions from the tetrahedral A-site with a non-magnetic ion such as

Zn will result in the reduction of the exchange interaction between Mn ions with Fe in the octahedral B-sites of the ferrite structure. Accordingly, a decrease in the Curie temperature and an increase in saturation magnetization can be expected [4].

The fact that Gd-ferrite exhibits a Curie temperature as low as 298K and high pyromagnetic coefficient could open the possibility to tune the T_c in Mn-Zn ferrites by a controlled incorporation of this rare-earth element in the host structure. Although this effect has been discussed [5], there is neither detailed evaluation nor discussion describing how the magnetization and pyromagnetic coefficient would depend on composition and crystal size in the Gd-doped systems. Our previous work has verified the effect of composition on the corresponding magnetization and demagnetization temperature in Gd-doped Mn-Zn ferrite nanocrystals synthesized through conventional coprecipitation method [6]. The present report addresses the development of a synthesis route that promotes growth of the ferrite crystals by controlling the oversaturation conditions during the ferrite formation in aqueous phase. It was expected that this enlargement of crystallite size should be conducive to an enhancement on the corresponding magnetization.

1 EXPERIMENTAL

1.1 Materials

All reagents were of analytical grade and were used without further purification. Required weights of chloride salts of Fe, Zn, Mn, and Gd ions were dissolved in distilled water to achieve a $[Fe+Gd]/M$ mole ratio two, ($M = Mn^{2+}+Zn^{2+}$). NaOH was used as the alkaline precipitant.

1.2 Synthesis of Ferrite Nanocrystals

Mn-Zn ferrite nanocrystals were produced by conventional and modified coprecipitation methods. Aqueous solutions of the metal ions were continuously added in to the reaction flask containing NaOH under boiling conditions. The Mn-Zn solution was prepared at various atomic fractions of Mn ions, 'x'. The atomic fraction of Gd species, 'y' was kept constant at 0.01 according to $Mn_xZn_{1-x}Fe_{2-y}Gd_yO_4$ stoichiometry. In the modified approach, the metal ions solution was contacted with the NaOH one at specific flow

rates (1mL/min to 20mL/min). Synthesized nanocrystals were removed out from solution, washed with deionized water three times and dried in air at 50 °C.

1.3 Characterization Techniques

Structural analysis of the powders were carried out in a Siemens D5000X-ray diffractometer (XRD) using the Cu-K α radiation. Magnetic properties of powders were measured in Lake Shore VSM magnetometer. Magnetization-temperature (M-T) curves were obtained under an external magnetic field 2.2T.

2 RESULTS AND DISCUSSION

2.1 XRD Analyses

XRD patterns for Mn_xZn_{1-x}Fe₂O₄ ferrites powders produced at various atomic fractions of Mn ions ('x'= 0.0-1.0) without control of flow-rate confirmed the formation of the ferrite structure. The average crystallite size, estimated by using the Debye-Scherrer's equation for the (311) peak, ranged from 6 nm to 15 nm when 'x' varied from 0 (zinc-ferrite) to 1.0 (manganese-ferrite) [6]. Figure 1 shows the XRD patterns for Mn_{0.8}Zn_{0.2}Fe₂O₄ powders produced after 1 hour of reaction. In these experiments, the Mn+Zn ionic solution was added into the NaOH one at a fixed flow-rate controlled by a peristaltic micro-pump. The flow-rate of the addition of reactants varied between 1mL/min and 20 mL/min. For comparison purposes, the pattern for the solid produced with no control on flow-rate ('0' mL/min) is also presented.

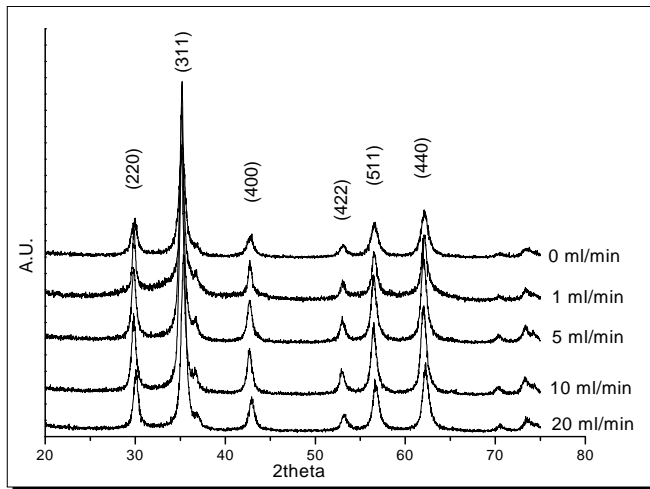


Figure 1. XRD patterns for Mn-Zn ferrites, 'x'= 0.8, synthesized at different flow-rates.

The corresponding average crystallite size varied from 15nm to 20nm when the flow-rate was increased from 1mL/min to 20mL/min, respectively. These values were larger than those determined for the ferrite synthesized with

no control on the flow rate; ferrite nuclei, quickly formed at the earlier stages of the reaction, would have acted as seeds, promoted heterogeneous nucleation and hence, crystal growth.

On the above basis, additional syntheses were carried out in presence of Gd (III) species under flow-controlled conditions. Figure 2 shows the XRD patterns for Mn_{0.8}Zn_{0.2}Fe_{1.99}Gd_{0.01}O₄ powders produced after 1 hour of reaction time and different flow-rates. Only peaks corresponding to the ferrite structure were observed when the flow-rate was 5mL/min or higher. However, two extra diffraction peaks centered on 22° and 34°, which could correspond to an isolated Gd-compound or ferrite precursor, were observed in the XRD pattern of the sample produced at 1mL/min. The low oversaturation condition attained at such a low flow-rate would have inhibited the incorporation of Gd species into the ferrite lattice. The average crystallite size varied from 12nm up to 18nm when the flow-rate was increased from 1mL/min to 20ml/min. The nanocrystals synthesized at 20ml/min exhibited an average crystallite size (18nm) larger than the one corresponding to the solid with the same composition but synthesized with no control of flow-rate (11 nm).

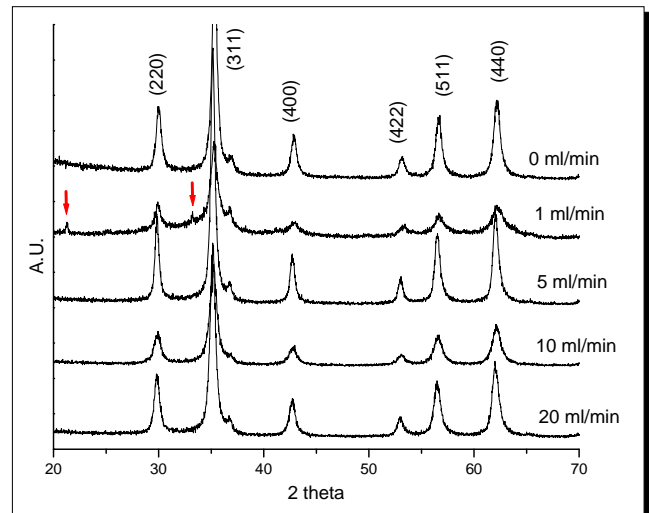


Figure 2. XRD patterns for Mn_{0.8}Zn_{0.2}Gd_{0.01}Fe_{1.99}O₄ powders synthesized at different flow rates.

2.2 Magnetic Measurements

M-H measurements were conducted on pure ('x'= 0.8), and Gd-doped, (y= 0.01), Mn-Zn ferrites synthesized at different flow-rates. The magnetization of pure MnZn ferrites exhibited a rising trend when the flow-rate was increased in the 1mL/min-20mL/min interval; the maximum magnetization was increased from 17emu/g up to 59emu/g (Figure 3). The rise in magnetization can be attributed to the larger size of ferrite nanocrystals, as suggested by XRD. The maximum magnetization for the

solid synthesized at the same composition but with no control on flow-rate ('0 mL/min') was 49emu/g.

Figure 4 shows the variation of magnetization with temperature for the Mn-Zn ferrite nanocrystals ($x' = 0.8$) synthesized at 20mL/min. The external magnetic field was 2.2 T. The T_c value, estimated by extrapolating the linear portion of the curve when the magnetization approached to zero, decreased from 675K (no control on flow-rate) down to 591K (20 mL/min). The corresponding pyromagnetic coefficient was increased from 0.16emu/g-K up to 0.34emu/g-K. Although still unclear, the drastic drop in T_c could be attributed to the change in the chemical composition of the ferrite when it is formed under flow-controlled conditions. Ongoing work using Mossbauer spectroscopy technique will provide additional insights on the actual reasons behind this behavior.

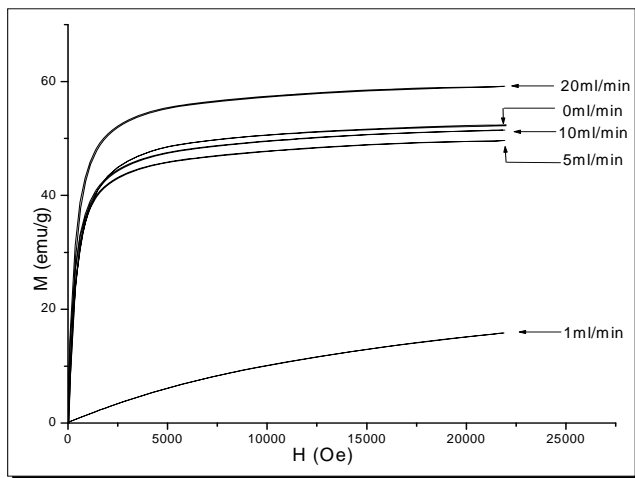


Figure 3. Room temperature M-H profiles for pure Mn-Zn ferrites ($x' = 0.8$) synthesized under flow-rate controlled conditions.

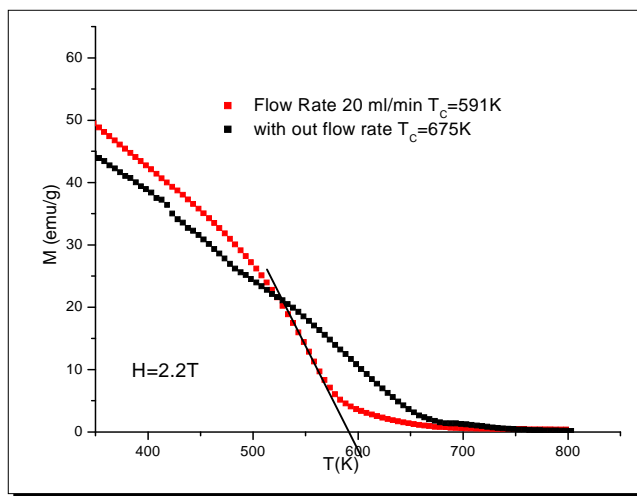


Figure 4. M-T profiles for pure Mn-Zn ferrites ($x' = 0.8$) synthesized with (20mL/min) and without control of flow-rate.

Previous data suggested that both, increase in magnetization and decrease in T_c could be achieved not only by suitable selection of the Mn-Zn ferrite composition but also by a suitable control of the flow-rate at which the reactants are added into the boiling NaOH solution. On this basis, the synthesis of Gd-doped MnZn ferrites was also carried out under flow-rate controlled conditions for a particular ferrite composition. The M-H profiles for Gd-doped Mn-Zn ferrite nanocrystals ($x' = 0.8$, $y' = 0.01$) are shown in Figure 5. The corresponding saturation magnetization values were increased (it varied from 20 emu/g up to 60 emu/g) when the flow-rate was augmented from 1mL/min to 20 mL/min. As discussed before, this variation in magnetization was attributed to the enhancement on crystal growth promoted by the higher flow-rates. Also here, the '0 mL/min' condition represents the M-H data for the ferrite synthesized with no control of the flow-rate.

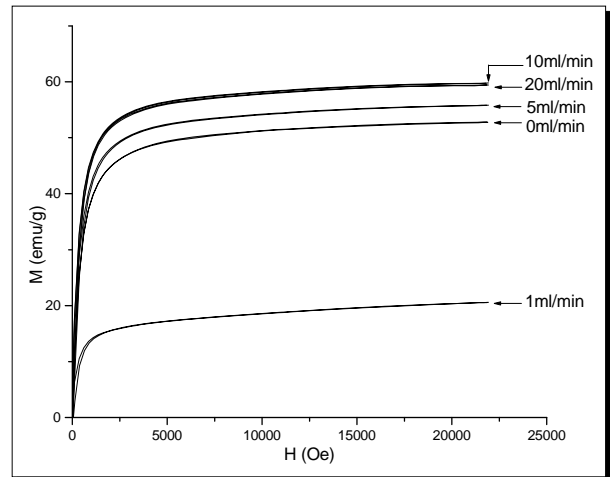


Figure 5. Room temperature M-H profiles for Mn-Zn ($x' = 0.8$) ferrites doped with Gd ($y' = 0.01$) and synthesized at different flow-rates.

Figure 6 compares the M-T profiles for pure ($x' = 0.8$, no control on flow-rate) and Gd-doped Mn-Zn ferrite ($y' = 0.01$) synthesized with (10ml/min) and without control of flow-rate. Although the T_c decreased from 675K to 604K, the corresponding magnetization did not exhibit noticeable variation under no flow-controlled conditions. The replacement of Mn ions by Gd ions at tetrahedral A-sites, which would have resulted in the reduction of the exchange interaction between Mn and Fe in the octahedral B-sites of the ferrite structure, could explain the drop in T_c [7, 8].

The control on flow-rate did not drastically affect the T_c of the Gd-doped ferrite, (it varied from 604K, no control on flow-rate, to 617K at 10ml/min). Furthermore, the doping of MnZn ferrite with Gd species was also conducive to the increase of the corresponding pyromagnetic coefficient from 0.15 emu/g-K (pure MnZn ferrite) to 0.27 emu/g-K, when the MnZn ferrite contained a Gd atomic fraction of 0.01.

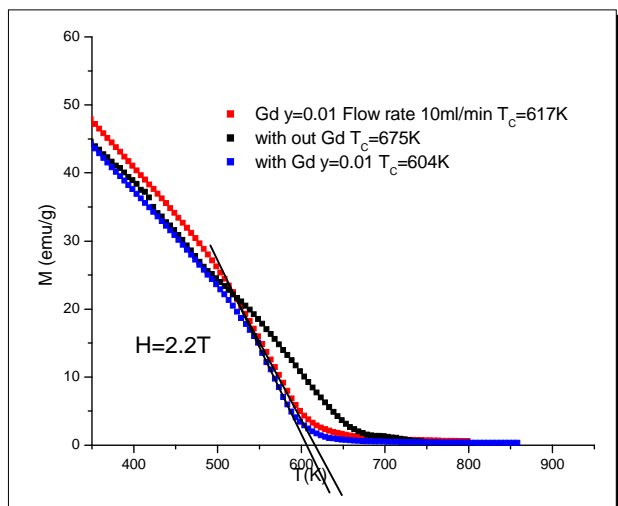


Figure 6. M-T profiles for pure ($x'=0.8$) and Gd-doped ($x'=0.8$, $y'=0.01$) MnZn ferrite nanocrystals synthesized with (10 mL/min) and without control on flow-rate.

3 CONCLUDING REMARKS

The simultaneous lowering of T_c while enhancing magnetization in MnZn ferrite nanocrystals, indispensable for magnetocaloric pumping applications, was achieved by proper selection of the ferrite composition (Mn and Gd atomic fractions of 0.8 and 0.01, respectively) and precise control of oversaturation conditions during ferrite formation in aqueous phase. The control of the flow-rate at which the reactants were mixed should have modified oversaturation conditions that promoted crystal growth and subsequent enhancement on magnetization. Under optimum conditions pure and Gd-doped Mn-Zn ferrite nanocrystals were enlarged from 11nm up to 18nm. The corresponding saturation magnetization values were 49emu/g and 60emu/g. Under no flow-controlled conditions, the probable incorporation of Gd species into the MnZn ferrite, ($x'=0.8$), made T_c to decrease from 675K to 604K. Ongoing work is focused on the use of Mossbauer spectroscopy to obtain additional insights about the observed magnetic behavior.

4 ACKNOWLEDGEMENTS

This material is based upon work supported by the US-Department of Defense under Award 50797 – RT-ISP.

REFERENCES

- [1] R.E. Rosensweig, *Ferrohydrodynamics*, Dover, New York, 1997.
- [2] L.J. Love, J.F. Jansen, T.E. Mcknight, Y. Roh, T.J. Phelps. A magnetocaloric pump for microfluidic

- applications. *IEEE Trans. Nanobiosci.* 3, 2, 101–110, 2004.
- [3] B. Jeyadevan, C.N. Chinnasamy, K. Shinoda, K. Tohji, Mn–Zn ferrite with higher magnetization for temperature sensitive magnetic fluid. *J Appl. Phys.*, 93, 8450-8452, 2003.
- [4] D. Zins, R. Massart, E. Auzans, E. Blums. Synthesis and properties of Mn–Zn ferrite ferrofluids. *J. Mater. Sci.* 34, 1253–1260, 1999.
- [5] R.V. Upadhyay, R.V. Mehta, Kinnari Parekh, D. Sriniva, R.P. Pant. Gd-substituted ferrite ferrofluid: a possible candidate to enhance pyromagnetic coefficient. *J. Magn. Magn. Mater.*, vol. 201, pp. 129-132, 1999.
- [6] E. Calderón-Ortiz, O. Perales-Perez and G. Gutierrez. $Mn_xZn_{1-x}Fe_{2-y}R_yO_4$ (R=Gd, Eu) ferrite nanocrystals for magnetocaloric applications. *Microelectron. J.*, doi:10.1016/j.mejo.2008.10.003, 2009.
- [7] Z. X. Tang, C. M. Sorensen, K. J. Klabunde. Size-dependent Curie temperature in nano-scale $MnFe_2O_4$ particles. *Phys. Rev. Lett.*, 67 1991.
- [8] N. Rezlescu, E. Cuciureanu, “Cation distribution and Curie temperature in some ferrites containing copper and manganese. *Phys. Status Solidi A*, 3, 873 – 878, 2006.